SHORT PREDICTING THE STRENGTH AND TOUGHNESS OF FIBER COMPOSITES

J.L. Kardos* and J.C. Halpin

Department of Chemical Engineering, Washington University, Campus Box 1198, One Brookings Drive, St. Louis, MO 63130, USA

SUMMARY: Predictions of strength and toughness for short-fiber-reinforced plastic systems are complex but industrially crucial problems. In this contribution, we utilize a new approach which accounts for the large stress concentration penalties in a perfectly aligned short-fiber composite. Although empirical, the approach permits calculation of a strength reduction factor which can then be utilized with an appropriate failure criterion to calculate the strength of a wide range of short-fiber composite systems. A similar approach is used for the toughness problem, with the fracture toughness of an isotropic, random-in-a-plane, short-fiber composite being expressed in terms of the fracture toughness of single unidirectionally oriented plies with cracks oriented along the two orthotropic axes. For both strength and toughness, a laminate analogy approach is used. The short-fiber system is thought of as being composed of several plies or layers, each containing uniaxially aligned short fibers. The plies are oriented in the laminate to replicate the actual system fiber orientation distribution, and the linear stress-strain or fracture toughness properties are calculated by analyzing the individual ply responses to the overall applied stress. Comparison with experimental data for random-in-a-plane fiber orientation and for biased in-plane orientations at practical fiber volume loadings shows good agreement. In the case of fracture toughness, there was qualitative agreement between theory and experiment, but the data scatter precluded a rigorous comparison.

INTRODUCTION TO THE STRENGTH PROBLEM

Prediction of strength for short-fiber-reinforced plastic systems is a complex but industrially crucial problem. Even in the case of unidirectionally aligned fibers with tensile stress applied in the fiber direction, failure may occur in the fibers, in the matrix phase, or at the interface. Furthermore, failure may take place in a tensile or shear mode and may be brittle or ductile in nature. The problem of strength prediction is best illustrated in Figure 1, wherein we see that unlike for stiffness, continuous-fiber composite strengths cannot be attained in discontinuous-fiber systems, even at very high aspect ratios. A second massive drop in strength occurs due solely to fiber orientation. Thus in going from a continuous aligned fiber system to a

 CCC 1022-1360/99/$ 17.50+.50/0

discontinuous, randomly oriented system, the strength has dropped by a factor of four. Any successful calculational format must account for both of these strength degradation phenomena.

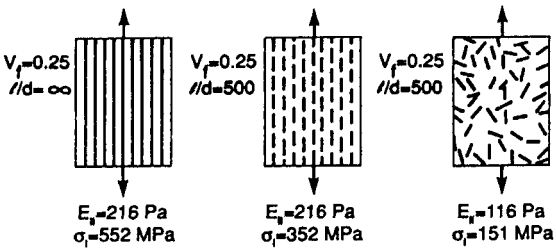

Figure 1.
The effect of fiber length and orientation on the mechanical properties of glass fiber epoxy composites.

It is appropriate at this point to discuss the upper bound for strength of an aligned fiber system; namely, the rule-of-mixtures expression for the strength in the fiber direction of an aligned continuous-fiber system (left-most system of Figure 1),

$$\sigma_c = \sigma_f V_f + c_m V_m \qquad (1)$$

where σ represents tensile strength, V is the volume fraction and the subscripts c, f, and m represent composite, fiber, and matrix, respectively. It is against this upper bound, in which fiber failure dominates, that aligned short-fiber system performance is conveniently compared. If the fibers have a wide distribution of strengths, which can occur due to fiber process variations or from fiber damage during composite fabrication, the statistics of fiber failure must be accounted for, as pointed out by Rosen (1).

STRENGTH OF UNIAXIALLY ALIGNED SHORT-FIBER SYSTEMS

Let us examine the first penalty in Figure 1, namely, the discontinuous nature of a perfectly aligned fiber system. Historically, the strength-of-materials approach to composite strength prediction began with the work of Cox (2) in 1952, which, although not exact, served as the basis for later developments of what is now called the "shear lag" analysis. Later detailed analyses by Dow (3) and Rosen (1) produced the same basic result. In 1964, Cottrell (4) formulated the basic shear lag analysis based on a single fiber and introduced the concept of a critical fiber length, l_{cr}, above which the fiber's ultimate strength will be fully utilized. One year later, Kelly (5-7) extended this principle to describe the behavior of short-fiber-reinforced metals and predicted that up to 95 % of continuous-fiber composite properties should be attainable with short-fiber systems if perfect uniaxial alignment is achieved. Unfortunately, perfectly uniaxial reinforcement is usually not attained experimentally. Lees attempted to

modify the shear large approach (8) by dividing the fiber length distribution into those fibers below and at or above the critical aspect ratio, and then summing the contributions to the two different failure modes. This approach also fails to predict experimental reality. Other approaches have been made from a strength-of-materials viewpoint (9).

More recently, Fukuda and Chou (10) developed a probabilistic theory which utilized the shear lag analysis and resulted in a modified rule of mixtures. No explicit attempt was made to compare with experimental strength values. Piggott (11) has also tried to modify the rule of mixtures by calculating factors based on forces necessary to pull out individual aligned fibers after a crack has passed across fibers and around fiber ends. Again, no agreement between predicted and experimental strength was shown. Chiang (12) has attempted a statistical theory for the tensile strength of short-fiber systems. He also used a modified rule of mixtures. His approach was similar to that of Lees (8), but he did not compare his predictions to experimental data and his expression for the strength of a planar random orientation is incorrect. Fu and Lauke (13) have attempted to extend Piggott's work (11). Their approach cannot explicitly predict experimental strengths because too many adjustable factors must be known. They showed agreement between calculated and experimental values for a lumped orientation/fiber length factor, but only after arbitrarily adjusting other factors. All of the efforts summarized above do not account for fiber end stress concentrations and their interaction. In the few instances of comparison to experiment, these approaches have failed to predict the strength of systems containing commercially important reinforcement levels.

It was not until the pioneering work of Chen in 1971 (14) that the interaction between neighboring short fibers was fully taken into account. Chen utilized a finite element approach, which included a distortional energy criterion, to calculate the strength of several uniaxially aligned short-fiber systems. He found that the composite strength reached a plateau as the fiber aspect ratio was increased at constant volume loading. Furthermore, this plateau occurred at only 80 % of the continuous-fiber value for tungsten-copper composites and at an incredibly low 55 % and 60 % of continuous values for boron-epoxy and glass-epoxy, respectively. Barker and MacLaughlin (15) and Riley (16) also concluded that interacting fiber stress concentrations should cause the strength to reach a plateau at large aspect ratios.

The only valid experimental claim of aligned short fibers attaining greater than 90 % of aligned continuous fiber properties is that of Dingle (17). In a carefully documented study in which the fiber alignment was demonstrably perfect, he showed measured mean tensile strengths in excess of 90 % of those for continuous composites of the same fiber volume

loading. Unfortunately, he used a tapered cross-section tensile specimen which has the effect of reducing scatter but also produces a single plane of maximum stress in which the probability of finding a fiber end approaches zero. In effect, a discontinuous-fiber specimen was transformed toward continuous-fiber behavior at the point of failure.

Schultrich et al. (18) developed a theory to predict the stress-strain behavior of short-fiber composites. They accounted for fiber-fiber interactions, but no comparison with experiment was provided. Hahn (19) has developed a strength-of-materials approach in which he accounts for stress concentrations via elastic stress partitioning. However, his equations require the empirical determination of stress concentration factors from data analysis. Unfortunately, he used data from Blumentritt et al. (20) whose specimens did not contain perfectly aligned fibers. Thus, Hahn's plots and analysis for unidirectional systems contain an orientation effect which could be quite large as we shall see. An equally system-dependent empirical approach was described by Bowyer and Bader (21).

Thus, it is clear that, unlike for stiffness, continuous-fiber composite strengths cannot be attained in unidirectionally oriented discontinuous-fiber systems, even at extremely high aspect ratios, because of fiber ends and fiber-fiber interactions. Furthermore, the critical aspect ratio, at which the maximum strength is achieved in short-fiber systems, is usually much higher than that needed to achieve the maximum (continuous-fiber) stiffness for the same fiber volume loading in the same system (22).

In this paper, we utilize a new approach which accounts for the large stress concentration penalties in a perfectly aligned short-fiber composite (23). Although empirical, the method permits calculation of a strength reduction factor, which can then be utilized with an appropriate failure criterion to calculate the strength of a wide range of short-fiber composite systems.

The strength of a uniaxially aligned, short-fiber composite may be predicted utilizing a strength reduction factor (SRF) approach developed by Halpin and Kardos (23, 24). The SRF is defined as the uniaxially aligned, short-fiber system strength divided by the strength of an aligned continuous-fiber system having the same volume fraction of fibers. Thus

$$[\mathrm{SRF}]_0 = \sigma_c/\sigma_R V_R \tag{2}$$

wherein the matrix contribution to the rule-of-mixtures continuous-fiber strength is neglected. σ_R is the fiber strength and V_R the volume fraction reinforcement. As the aspect ratio approaches unity, the [SRF] approaches that for a sphere-filled system, namely $[\mathrm{SRF}]_0$. This

lower bound can be evaluated by utilizing the results of Narkis et al. (25-27) for glass-bead-filled thermoplastics and thermosets (σ_m is the matrix strength):

$$[\mathrm{SRF}]_0 = \frac{\sigma_m E_c \left(1 - V_R^{1/3}\right)}{\sigma_R V_R E_m} \tag{3}$$

The value for the [SRF] at large fiber aspect ratios, $[\mathrm{SRF}]_\infty$, may be shifted vertically by utilizing the fiber-to-matrix stiffness ratio, E_R/E_m, which in fact controls the magnitude of the stress concentrations at the fiber ends (14-16). The best fit for this shift yields

$$[\mathrm{SRF}]_\infty = 0.5 + \left(E_R/E_m\right)^{-0.87} \quad \text{for } E_R/E_m > 5 \tag{4}$$

The horizontal shift parameter, β, can be developed by noting the parameters of importance in the shear lag analysis. The critical aspect ratio and the ratio of fiber strength to matrix shear strength are related by a constant. Thus the horizontal shift parameter is

$$\beta = \left(l/d\right)/\left(\sigma_R/\tau_m\right) \tag{5}$$

where τ_m is the shear strength of the interface or matrix, whichever is lower.

The final equation for the master curve may be normalized and expressed as follows:

$$G = \frac{[\mathrm{SRF}] - [\mathrm{SRF}]_0}{[\mathrm{SRF}]_\infty - [\mathrm{SRF}]_0} = 1 - 0.97 \exp\left[-0.42\beta\right] \tag{6}$$

The above equations, collectively denoted as the Halpin-Kardos equations, predict the lowering of continuous-fiber strength due to the discontinuous nature of the reinforcement. Figure 2 presents a nonlinear regression fit of finite element calculations using Chen's approach (14). For each experimental data set, a finite element curve was calculated and expressed in terms of Halpin-Kardos equation parameters.

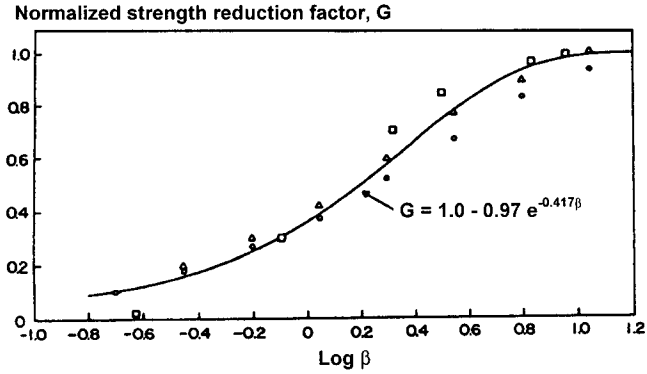

Figure 2.

Best fit of Halpin-Kardos equations to experiment-based finite element results (from Ref. 24).

□ W/Cu (T =300 °C)

○ E-glass/epoxy

△ boron/epoxy

Points from these individual curves are plotted in Figure 2 and the solid line represents a second nonlinear regression fit of the points to determine the best values for the constants of the Halpin-Kardos equation. This equation also fits the experimental data for both ductile (28) and brittle (29) epoxy matrices reinforced with E-glass fibers.

The fiber volume fraction appears explicitly only in the expression for $[SRF]_0$. Since all of the fitting was done using a fiber volume fraction of 0.5, it is important to examine the effect of fiber volume fraction on $[SRF]_\infty$. Since there was not enough well characterized experimental data available at other volume fractions, the finite element approach utilized by Chen (14) was used to calculate the effect of fiber loading on $[SRF]_\infty$; at ratios of E_f/E_m larger than 100, the effect was found to be quite small and may be neglected for practical design considerations (22).

THE LAMINATE ANALOGY FOR STRENGTH EFFECT OF FIBER ORIENTATION

The second portion of the strength calculational format portrays the short-fiber-reinforced part as being composed of several plies or layers, each containing uniaxially aligned short fibers. The plies are oriented in the laminate to replicate the actual part fiber orientation distribution and the linear stress-strain properties are calculated by analyzing the individual ply responses to the overall applied stress. The general procedure will now be outlined:

1. The first step requires the choice of a failure criterion for a continuous-fiber-reinforced ply having uniaxial orientation. One such criterion holds that if the ply is strained beyond certain maximum values in tension and shear, the ply will fail. This maximum strain criterion has been shown to work quite well (23) in brittle matrix systems and will be used in this format; however, any other failure criterion (30,31) could alternatively be chosen. Experimental values for the allowable maximum strains must be determined for the system of interest for transverse (to the fibers) tension, longitudinal tension, and in-plane shear.

2. For each ply at its particular orientation in the laminate, the applied strains are transformed from the axial direction of the laminate to the principal directions of the ply. The smallest axial strain that will cause failure of the ply is noted and the order of the ply failure is thus determined. Once the first-ply failure axial strain is known, this is assumed to be the midplane strain of the laminate and the stress causing that failure can be calculated.

3. The next step is to calculate the plane stress moduli of the individual uniaxially oriented plies and then transform them to the particular orientations occupied by the plies in the laminate. These transformed moduli are then summed through the layers of the laminate

thickness and the overall effective engineering moduli of the laminate calculated. If the part being analyzed is a random-in-a plane sheet, there will be eight plies, two at each of 0°, + 45°, – 45°, and 90° angles. For a nonrandom orientation, the number of plies and their thicknesses will depend on the angular increments chosen to divide up the distribution.

As a first trial, the order of ply failure can be assumed to be the same as the continuous-fiber case and the laminate stiffnesses recalculated by deleting the failed ply from the laminate.

4. Next, the allowable strains for the continuous-fiber ply must be reduced to account for the short-fiber penalty. This is conveniently accomplished using the Halpin-Kardos equations which yield a strength reduction factor (SRF) which, along with the moduli of the short-fiber and continuous-fiber systems, permits calculation of the allowable strains for the short-fiber system.

   This reduction may change the order of ply failure compared to that for the continuous-fiber case. If that occurs, then the laminate stiffnesses will have to be recalculated as a function of the correct ply failure order. The transformation of the allowable strains will also have to be recalculated because the Poisson ratio also will depend on the order of ply failure. An example of this phenomenon is illustrated in Appendix II of Ref. 22.

5. The calculation continues by utilizing the increments between the failure strains and the recalculated overall laminate stiffnesses. The lowest transformed axial allowable strain is chosen and the incremental stress needed to produce this incremental strain is calculated using the applicable stiffness. The second failed ply is deleted and the calculation is repeated. After all the plies have failed, the incremental strains and stresses are summed to obtain the ultimate stress and strain of the laminate.

The necessary equations and an example for random-in-a-plane orientation, are described in detail in Ref. 22.

Following the format outlined above, the uniaxial tensile strength of a random-in-a-plane orientation, E-glass/epoxy composite may be predicted. The calculational details have been presented elsewhere (22) and only the salient results are summarized here. For a 50 vol.-% fiber loading, the stress-strain results are summarized in Table 1. Note that the 90° ply failed first, followed by the 0° plies, and then the $\pm 45°$ plies. Note also that as the plies fail, the laminate stiffness decreases yielding a piece-wise linear stress-strain curve. While the

experimental curve does not look like this, the ultimate stress and strain agree well with experiment.

Table 1 Stress-strain results for E-glass/epoxy composite with 50 wt.-% fiber loading

Ply failure	ε_x	E psi (GPa)	$\Delta\varepsilon_x$	$\Delta\sigma_x = E\Delta\varepsilon_x$ psi (MPa)	$\sum \Delta\sigma_x$ psi (MPa)
90°	0.0038	2.67×10^6 (18.4)	0.0038	10 000 (68.9)	10 150 (69.9)
0°	0.126	2.13×10^6 (14.7)	0.0118	25 130 (173)	35 280 (243)
±45°	0.0205	0.74×10^6 (5.10)	0.0049	3 630 (25.0)	38 910 (268)

Figure 3 shows the predicted strength for a random-in-a-plane fiber orientation, along with experimental data from a brittle matrix, glass/epoxy system (32). The prediction provides a reasonably good (and conservative) engineering estimate of the strength. Reasonable predictions using the above approach have also been achieved for nonrandom orientation (33).

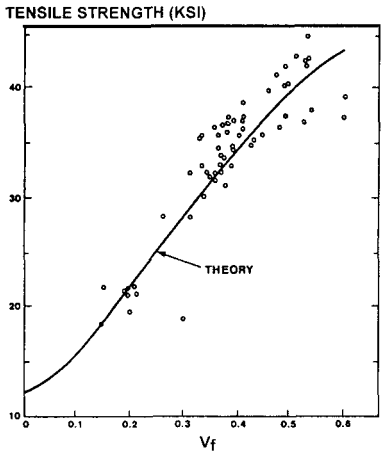

Figure 3.

Theory utilizing the laminate analogy and maximum strain failure criterion (solid line) compared with experimental data for two-dimensional random fiber ($L/D > 500$) orientation in a brittle glass-epoxy matrix.

The fact that the prediction is still somewhat below experiment may be due to (a) the incremental stresses and strains not being additive because of path-dependent effects caused by ply failure, (b) lack of information on how ply failure strains vary with fiber volume fraction, and (c) failure to retain at least the shear components of the ply stiffness matrix after ply failure.

A number of investigators have attempted to average the off-axis angular strength dependence of a unidirectional ply by integrating a piece-wise continuous function over 90° (8,12,14,34). In each case, agreement with experimental data was poor. The concept of integrating through the thickness to average the effects of different failure mechanisms is theoretically questionable, particularly if uniform strain is invoked via the maximum-strain-failure criterion.

There are a number of important issues which emanate from the above approach. The degree of adhesion is extremely important and is reflected in an interface strength term. This term is not predictable and is extremely difficult to measure experimentally (35). The use of single-fiber pull-out tests may be misleading because these results do not account for the very important fiber-fiber interactions in the composite. The strength of flaw-sensitive fibers such as glass is dependent on fiber length and the intrinsic strength of the actual short fiber must be used in any predictive format. The three-dimensional short-fiber strength problem has barely been touched and will certainly become a more important issue as these systems head toward uses as primary structural materials.

INTRODUCTION TO THE TOUGHNESS PROBLEM

The fraction toughness of polymer composites is probably one of the least understood of all the mechanical responses. For most composites, including short-fiber systems, a sometimes espoused rule of thumb is that as the strength increases, the toughness decreases. Thus, it might be implied that as the degree of adhesion increases, the toughness should decrease. While this is true generally for continuous-fiber-reinforced brittle matrices, it is not always the case for particulate filled systems (36), nor for short-fiber-reinforced thermoplastics (37).

Figure 4 qualitatively summarizes some of the results obtained by DiBenedetto (37-39).

Improving the adhesion in a short glass fiber/poly(phenylene oxide) system actually increases the fracture toughness as measured in a double-edge-notched tensile test. Friedrich (40) has presented similar findings for a variety of thermoplastic matrix systems. The same trend is clear in the glass bead/PPO system. Thus, the reinforcement geometry, the fiber-matrix adhesion, and the matrix ductility are important fracture toughness considerations. Gaggar and Broutman (41) measured the crack growth resistance of single-edge-notched tensile specimens of chopped glass/polyester mats. They found that the crack growth resistance increased as the crack grew. Working also with chopped glass strand/polyester mat, Owen and Bishop (42) found that the critical stress intensity factor increased with crack length.

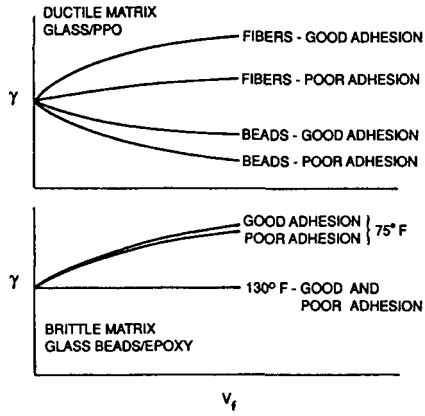

Figure 4.

Qualitative effects of reinforcement geometry, matrix ductility, degree of adhesion, and volume loading on the fracture toughness of glass-reinforced plastics.

Although various attempts have been made to increase toughness by adding a ductile-third-phase material, either dispersed in the matrix or selectively located at the interface, there is still no good format for predicting, *a priori*, the toughness of a composite system. A start toward this goal has recently been made by Lauke et al. (43) who have attempted to develop a theoretical micromechanical interpretation of fracture work in short-fiber-reinforced thermoplastics. Although their approach is a good start, it neglects fiber interaction.

PREDICTIVE FORMAT FOR FRACTURE TOUGHNESS

The approach to predicting toughness described herein is based on the same micro- and macromechanical analysis (commonly referred to as a laminate analogy) used for the strength problem. A random-in-a-plane short-fiber-reinforced sheet may be modeled as a quasi-isotropic laminate ($0°$, $\pm 30°$, $\pm 60°$, $90°$) composed of individual plies each of which contains perfectly unidirectionally oriented short fibers. Micromechanics is used to predict the behavior of each individual, unidirectionally oriented ply and the individual ply responses are then summed using macromechanics lamination theory. This approach will now be presented briefly and the essential equations outlined. A more detailed development of the equations appears in Ref. 44.

The fracture toughness of an isotropic material as well as for the orthotropic directions of a unidirectionally oriented composite is given (37,45) in terms of the Mode 1 critical stress intensity factor, K_{Icr}, and the effective stiffness, E_{eff} as shown in Eq. 7.

$$\gamma_{Icr} = \frac{K_{I\,cr}^2}{2E_{eff}} \tag{7}$$

Expressions for the effective stiffness exist in terms of the components of the stiffness, the compliance and the engineering constants (44-46). For an isotropic laminate, the effective value of the modulus coincides with the Young's modulus, while for orthotropic laminates, Eqs 8 and 9 apply.

$$E_{\text{eff}_1} = \left(2\overline{E}_{11}\overline{E}_{22}\right)^{1/2} \Bigg/ \left[\left(\frac{\overline{E}_{22}}{\overline{E}_{11}}\right)^{1/2} - \overline{\nu}_{21} + \frac{\overline{E}_{22}}{2\overline{G}_{12}}\right]^{1/2} \tag{8}$$

$$E_{\text{eff}_2} = \left(2\overline{E}_{11}\overline{E}_{22}\right)^{1/2} \Bigg/ \left[\left(\frac{\overline{E}_{11}}{\overline{E}_{22}}\right)^{1/2} - \overline{\nu}_{12} + \frac{\overline{E}_{11}}{2\overline{G}_{12}}\right]^{1/2} \tag{9}$$

where $E_{\text{eff}_1}, E_{\text{eff}_2}$ are effective Young's moduli for double-edge-notched specimens notched perpendicular and parallel to the fiber direction, respectively; $\overline{E}_{11}, \overline{E}_{22}$ are Young's modulus for the longitudinal (parallel to the fibers) and transverse directions for a unidirectional ply; $\overline{\nu}_{12}, \overline{\nu}_{21}$ are longitudinal (major) and transverse (minor) Poisson's ratio; $\overline{G}_{12}$ is in-plane shear modulus.

The above engineering constants may be calculated using the Halpin-Tsai equations (47). The critical stress intensity factor, K_{Ic}, is given by Eq. 10.

$$K_{I\,\text{cr}} = \sigma_n\sqrt{\pi c_{\text{eff}}} = \sigma_n\sqrt{\pi\left(c + 2v_{\text{cr}}\right)} = \sigma_1\sqrt{2\pi r_{\text{cr}}} \tag{10}$$

K_{Ic} from Eq. 4 must be corrected for specimen dimensions by the following factor (45).

$$F\left(\frac{c_{\text{eff}}}{b}\right) = \left[\frac{2b}{\pi c_{\text{eff}}}\tan\frac{\pi c_{\text{eff}}}{2b}\left(1 + 0.2\cos^2\frac{\pi c_{\text{eff}}}{2b}\right)\right]^{1/2} \tag{11}$$

where σ_n = notched strength, σ_1 = tensile strength, r_c = latent material flaw, b = half specimen width, c = half crack length, $c_{\text{eff}} = c + 2r_c$.

The final expression for the opening Mode 1 critical stress intensity factor is

$$K_{I\,\text{cr}} = \sigma_n\left\{2b\left[\tan\frac{\pi\left(c + K_{I\,\text{cr}}^2/2\pi\sigma_1^2\right)}{2b} + 0.1\sin\frac{\pi\left(c + K_{I\,\text{cr}}^2/2\pi\sigma_1^2\right)}{b}\right]\right\}^{1/2} \tag{12}$$

The above equation can be solved for K_{Ic} using the bisection iteration method. The theoretical value of the tensile strength, σ_1, for a perfectly oriented ply is calculated by employing the Halpin-Kardos equations described above.

The value for σ_1 may also be measured experimentally on an unnotched, unidirectionally oriented short-fiber ply, although such a ply is extremely difficult to fabricate.

The notched strength for a specimen with the cracks oriented perpendicular to the direction of the fibers is obtained from the modulus calculated via Eq. 7 and the experimentally measured strain at failure, or directly from the experimental notched strength. In either case, if the fibers are not perfectly oriented, a correction must be applied so that a value for perfect alignment results.

For the case in which the notches are aligned in the same direction as the fibers, the notched strength of the matrix was employed. That is definitely an upper bound since the crack can sometimes propagate through the fiber bundles at interfaces, resulting in a much lower notched strength. The fracture toughness (fracture surface energy), γ_R, of an isotropic composite laminate made of plies can be expressed in terms of the fracture toughnesses of an orthotropic laminate (a single unidirectionally oriented ply), with the cracks oriented along the two axes of orthotropy (44).

$$\gamma_R = \frac{\gamma_1 + \gamma_2}{n \sin \frac{\pi}{2n}} \left[\frac{\sin\left(\frac{\pi}{4} + \frac{\pi}{2n}\right) + \cos\left(\frac{\pi}{4} + \frac{\pi}{2n}\right)}{\sqrt{2}} \right] \tag{13}$$

The angle between two successive plies is π/n.

For large n (> 100),

$$\gamma_R = \frac{2(\gamma_1 + \gamma_2)}{\pi} \tag{14}$$

γ_1 and γ_2 are obtained by applying Eqs 6-11 to a single unidirectionally oriented ply with the notches oriented parallel and perpendicular to the fiber direction.

Thus, one can start from the engineering constants of the matrix and the fibers, as well as the aspect ratio and volume fraction of the fibers, and characterize the unidirectional ply. One can then determine the engineering constants, strength, and fracture toughness of the quasi-isotropic laminate, which is equivalent to the random-in-a-plane short-fiber composite, using lamination theory and the above equations.

Figure 5 shows the predicted toughness values (solid lines) for two different fiber volume fractions for random-in-a-plane fiber orientation in a glass/epoxy system. Also shown are the experimental data which contain considerable scatter. The predictions indicate a weak critical aspect ratio effect although the experimental scatter makes it difficult to corroborate this

prediction. Details of the specimen preparation, characterization, and calculations are presented in Ref. 48.

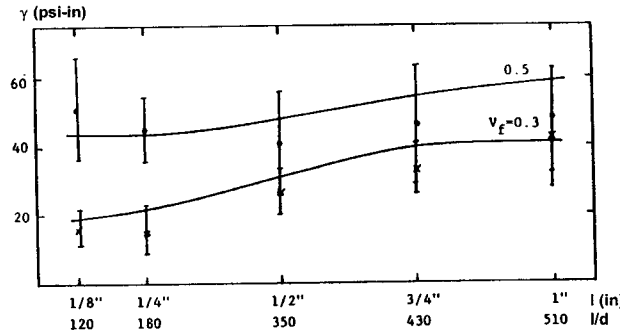

Figure 5.
Fracture toughness versus fiber bundle length for isotropic laminate (EPON 828-Z).

The first important point is that the data scatter is quite large as is usually the case for toughness measurements. Thus, it is difficult to say whether or not the predicted and experimental values match. The upward trend of γ_{Icr} as the aspect ratio increases looks a little like the strength dependency and, at a volume loading of 0.3, the predictions follow the data reasonably well. However, at a V_f of 0.5, one might argue that the experimental toughness drops slightly or is constant as the bundle aspect ratio rises, whereas the predicted curve shows a slight rise.

The fracture surface energy, γ_{Icr}, by definition is the stored elastic strain energy per unit area of fracture surface during the initiation of the crack. The highest value for γ_{Icr} for the brittle matrix system was about 60 in-lbs/in^2, whereas a ductile matrix system produced values as high as 160 in-lbs/in^2 (48). In both cases, increasing the fiber volume content caused an increase in fracture surface energy. This is most likely due to the more tortuous crack path required in the more highly loaded system.

Fractography, primarily with the scanning electron microscope, indicated first of all that the adhesion was excellent. Secondly, cracking took place primarily around the bundles, rather than through them. Little evidence of fiber breakage was seen except for the 1-inch bundles where the crack was also seen to often penetrate the bundles. Again, the scatter in the data is too large to identify a critical bundle aspect ratio for toughness. Theory suggests that such a phenomenon should exist as a result of similar behavior for both stiffness and strength.

Use of the laminate analogy for toughness assumes that one can combine the toughness contribution of a crack moving initially perpendicular to the fibers with that of a crack moving initially parallel to the fibers. Certainly, both phenomena must occur for a random-in-a-plane orientation. The real question lies in whether or not one can add these responses

volumetrically through a laminate analogy or whether some other weighting law is obeyed. The data from this study are not sufficient to answer that question.

CONCLUSIONS

The combined use of micromechanics to yield the unidirectional short-fiber response along with the macromechanics (laminate analogy) to account for fiber orientation is a successful format for predicting the stiffness, strength, and fracture toughness of short-fiber composites with planar, two-dimensional fiber orientations This approach properly accounts for the major short-fiber penalty of interacting fiber and stress concentrations, as well as interfacial adhesion, aspect ratio, volume fraction fibers, fiber orientation distribution, and fiber and matrix mechanical properties. More work needs to be done to successfully predict the properties of three-dimensionally oriented fiber composites.

REFERENCES

1. W. Rosen, "Mechanics of Composite Strengthening" in *Fiber Composite Materials*, American Society for Metals, Metals Park, OH, 1965, Chap. 3
2. L. Cox, *Br. J. Appl. Phys.* 3, 72 (1952)
3. F. Dow, General Electric Report R635D61 (1963)
4. H. Cottrell, *Proc. R. Soc. London, Ser. A* 282, 2 (1964)
5. Kelly, Fibre Reinforcement, in "Strong Solids", Clarendon Press, Oxford (1969)
6. Kelly and W. R. Tyson, *J. Mech. Phys. Solids* 13, 329 (1965)
7. A.Kelly and G. J. Davies, *Metall. Rev.* 10, 1 (1965)
8. K. Lees, *Polym. Eng. Sci.* 8,195 (1968)
9. O. Outwater, Jr., *Mod. Plast.* 33, 156 (1956)
10. Fukuda and T. W. Chou, *J. Mater. Sci.* 17, 1003 (1982)
11. R. Piggott, *J. Compos. Mater.* 28, 588 (1994)
12. R. Chiang, *Compos. Sci. Technol.* 50, 479 (1994)
13. Y. Fu and B. Lauke, *Compos. Sci. Technol.* 56, 1179 (1996)
14. E. Chen, *Polym. Eng. Sci.* 11, 51 (1971)
15. M. Barker and T. F. MacLaughlin, *J. Compos. Mater.* 5, 492 (1971)
16. R. Riley, *J. Compos. Mater.* 2, 436 (1968)
17. E. Dingle, *Proc. Int. Conf. On Carbon Fibers, Their Place in Modern Technology*, The Plastics Institute, London, 1974, paper No. 11
18. Schultrich, W. Pompe, H. J. Weiss, *Fiber Sci. Technol.* 11, 1 (1978)
19. T. Hahn, in *Composite Materials in the Automobile Industry*, S. V. Kulkarni, C. H. Zweben, R.B. Pipes, Eds., ASME, New York, 1978, p. 85

20. F. Blumentritt, B. T. Vu, S. L. Cooper, *Polym. Eng. Sci.* 14, 633 (1974)

21. H. Bowyer, M. G. Bader, *Mater. Sci.* 7, 1315 (1972)

22. L. Kardos, "Mechanical Properties of Polymeric Composite Materials," in *High Performance Polymers*, E. Baer and A. Moet, Eds, Hanser Publ., Munich, p. 199 (1991)

23. C. Halpin, J. L. Kardos, *Polym. Eng. Sci.* 18, 496 (1978)

24. L. Kardos, J. C. Halpin, S. L. Chang, in *Rheology*, Vol. 3, G. Astarita, G. Marrucci, L. Nicolais. Eds, Plenum, New York, 1980, p. 225

25. E. Lavengood, L. Nicolais, M. Narkis, *J. Appl. Polym. Sci.* 17, 1173 (1973)

26. Narkis, *Polym. Eng. Sci.* 15, 316 (1975)

27. Narkis, *J. Appl. Polym. Sci.* 20, 1597 (1976)

28. Masoumy, L. Kacir, J. L. Kardos, *Polym. Compos.* 4, 64 (1983)

29. Kacir, M. Narkis, O. Ishai, *Polym. Eng. Sci.* 17, 234 (1977)

30. W. Tsai, E. M. Wu, *J. Compos. Mater.* 5, 58 (1971)

31. L. Kardos, *Crit. Rev. Solid State Sci.* 3, 419 (1973)

32. E. Lavengood, *Polym. Eng. Sci.* 12, 48 (1972)

33. L. Kardos, E. Masoumy, L. Kacir, in *The Role of the Polymeric Matrix in the Processing and Structural Properties of Composite Materials*, J. C. Seferis, L. Nicolais, Eds., Plenum Press, New York, 1983, p. 407

34. T. Hahn, *J. Compos. Mater.* 9, 316 (1975)

35. R. Piggott, *Polym. Compos.* 3, 179 (1982)

36. Bramuzzo, A. Savadori, D. Bacci, *Polym. Compos.* 6, 1 (1985)

37. Wambach, K. Trachte, A. T. DiBenedetto, *J. Compos. Mater.* 2, 266 (1968)

38. T. DiBenedetto, A. D. Wambach, *Int. J. Polym. Mater.* 1, 159 (1972)

39. L. Trachte, A. T. DiBenendetto, *Int. J. Polym. Mater.* 1, 75, (1971)

40. Friedrich, *Compos. Sci. Technol.* 22, 43 (1985)

41. K. Gaggar and L. R. Broutman, *Adv. Chem. Ser.* 154, 355 (1976) (Toughness and Brittleness of Plastics)

42. J. Owen and P. T. Bishop, *J. Compos. Mater.* 7, 146 (1973)

43. Lauke, B. Schutrich, R. Bauthel, *Compos. Sci. Technol.* 23, 21 (1985)

44. Tsarnas, "Fracture Toughness of Short Fiber Reinforced Composites," D.Sc. Thesis, Washington University, 1982

45. R. Irwin, "Fracture Testing of High Strength Sheet Materials Under Conditions Appropriate for Stress Analysis," U. S. Naval Lab., Washington, DC, NLR Report #5486, 1960

46. C. Sih, P. C. Paris, and G. R. Irwin, *Int. J. Fract. Mech.* 1, 189 (1965)

47. C. Halpin, *Primer on Composite Materials: Analysis*, 2nd ed., Technomic, Lancaster, PA, 1984

48. Tsarnas, J. L. Kardos, Proc. 43rd Annu. Conf. SPE, 31, 377 (1985)